# Characterization of Highly Doped Si Through the Excitation of THz Surface Plasmons

Maxim M. Nazarov, Alexander P. Shkurinov, Frédéric Garet, and Jean-Louis Coutaz

***Abstract*—We excite surface plasmons (SPs) at the surface of highly doped Si using a prism coupler, and we study the propagation properties of these SPs in order to characterize the terahertz (THz) response of the doped semiconductor. Thanks to the long interaction length of the propagating SP with the substrate material, the method is more sensitive than classical THz time-domain spectroscopy in reflection or in transmission. Moreover, we propose a new technique based on measuring the SP signal, for which the delicate problem of accurately measuring the phase of the signal is solved. All of these different experiment techniques allow us to determine reliably the dielectric function of highly doped Si in the THz range. It appears that the experimentally determined values differ strongly from the ones calculated with a Drude model.**

***Index Terms*—ATR, dielectric function, doped silicon, Drude model, semiconductor, surface plasmon.**

## I. Introduction

In the far-infrared and terahertz (THz) spectral regions, metals and doped semiconductors obey fairly well to the classical Drude model [1], in which free carriers do not interact with other carriers and with the material lattice (at least, the interaction with the lattice is simply accounted by using the effective mass of the carriers). The oscillation of the carriers with the THz field is only damped by collisions against structural defects, impurities, or, more likely, phonons at room temperature. Nevertheless, it appeared during the last decades that more sophisticated models are necessary to describe the far-infrared properties of highly conducting materials that can be measured by THz time-domain spectroscopy (TDS). Grischkowsky and coworkers reported a comprehensive study of doped silicon, with $n$ and $p$ doping densities $N$ varying within the range $10^{14} - 10^{16}$ cm$^{-3}$ [2], and later they show that the Cole–Davison model [3], which combines both Drude and Debye approaches, provides an even better fit of the experimental data. More recently, Lloyd-Hughes [4], [5] solved numerically the Boltzmann equation in the relaxation time approximation to derive the THz conductivity of polar semiconductors like GaAs or InAs. Because the free carrier scattering depends on the energy, the agreement between experiment and theory is excellent. For $n$-doped GaAs, the Boltzmann theory and the Drude model differ only in terms of the imaginary part of the conductivity at higher energy, i.e., typically over 0.5 THz. Simultaneously, Willis *et al.* [6], [7] have used a Monte-Carlo simulation of the carrier transport, together with a finite-difference time-domain calculation of the coupling with the Maxwell's equations, to determine the THz response of doped silicon. The model fits well experimental data by Jeon and Grischkowsky [8]. Here again, the difference with the Cole–Davison model is rather tiny.

Characterizing the electromagnetic response, i.e., the complex permittivity or the complex index of refraction, of metals or highly doped semiconductors in the far infrared is a difficult task, because of the large value of their permittivity. Thus transmission measurements are not possible unless very thin samples are used: unfortunately, due to free carrier confinement effects, the response of thin (tens of nanometers) films differs from the bulk one [9], [10]. Characterization in reflection configuration [3], [11], where the material serves as a mirror, is preferable, but the method is not sufficiently sensitive to deliver an accurate determination of the material permittivity. A better solution is to perform THz ellipsometry [12], [13]. In addition, high-$Q$ cavity measurements were used to extract doped Si properties [14], [15] in the sub-THz range (0.3–1 THz), these deviations were also numerically calculated in [6] for $N = 5 \times 10^{14}$ cm$^{-3}$ doping concentration.

We present here another technique based on the excitation of THz plasmons (SP) at the surface of the material. Experimental study of THz SPs on semiconductors was reported in a few papers. SPs were excited on Si using a grating coupler [16], on InAs with an attenuated total reflection scheme (ATR—Otto prism configuration) [17], on porous Si [18], and InSb [19] through edge excitation or using a subwavelength slit [20]. Analytical estimations of SP confinement and propagation on doped Si ($N = 10^{20}$ cm$^{-3}$) and on gold are presented in [21] over a broad frequency range, including the THz domain.

As semiconductors exhibit a plasma frequency that depends on the electron density, the properties of SPs propagating over a semiconductor can be tailored within the THz range through doping or photoexcitation [22]. Semiconductors with low collision frequency and high mobility, like InSb [19], are good materials for THz SP devices, but they are difficult to obtain. On the other hand, Si is a widely spread material that supports THz SP when doped above $N = 10^{17}$ cm$^{-3}$.

In this work, we demonstrate broadband THz SP propagation on a highly doped Si wafer. We investigated the SP properties using known methods (reflection spectroscopy and ATR angular measurements) as well as using our new method based on SP transmission spectroscopy. Only this last method is sufficiently

Manuscript received April 08, 2015; revised June 08, 2015; accepted June 08, 2015. Date of publication July 09, 2015; date of current version July 16, 2015. The work of M. M. Nazarov was supported by RFBR under Grant 14-02-00846.

M. M. Nazarov is with the Institute on Laser and Information Technologies RAS, Shatura140700, Russia (e-mail: nazarovmax@mail.ru).

A. P. Shkurinov is with Department of Physics, M.V. Lomonosov Moscow State University, Moscow 1119992, Russia.

F. Garet and J.-L. Coutaz are with IMEP-LAHC, UMR 5130 CNRS, Université de Savoie, 73376 Le Bourget du Lac, France.

Digital Object Identifier 10.1109/TTHZ.2015.2443562

2156-342X © 2015 IEEE. Personal use is permitted, but republication/redistribution requires IEEE permission.
See http://www.ieee.org/publications_standards/publications/rights/index.html for more information.

sensitive to obtain surface dielectric function spectra. The so-determined dielectric function of doped Si differs strongly from the one given by the Drude theory.

## II. Requirements for Doped SI to Support THZ SP

The dielectric function of bulk doped semiconductor is fairly well described by the Drude model [5]

$$\varepsilon(f,N,d)=\varepsilon_\infty-\frac{f_p(N)^2}{f^2+i\Gamma_d f} \tag{1}$$

where $f$ is the frequency, $\Gamma_d$ is the collision rate, and $f_p=(1/2\pi)\sqrt{(N\,e^2/\varepsilon_0 m_d^*)}$ is the plasma frequency. Subscript $d$ denotes either $n$ or $p$ doping type. For the case of Si, $\varepsilon_\infty=11.7$, and the free carrier effective mass is $m_p^*=0.37\,m_e$, and $m_n^*=0.26\,m_e$. Carrier concentration $N$ is the only variable that determines the Si optical response. Often, dc mobility $\mu$ is used to characterize semiconductors, which is related to the preceding parameters as $\Gamma_d=(e/\mu_d m_d^*)(1/2\pi)$ [8]. For Si, $\mu$d is in the range 300–1000 $\mathrm{cm}^2/(\mathrm{V}\cdot\mathrm{s})$. Note that mobility $\mu$ and accordingly collision rate $\Gamma_d$ change with carrier concentration [8], [23] and temperature [12], and they depend on doping type. For example, for $N=9\times10^{16}$ $\mathrm{cm}^{-3}$, $\Gamma_p=1.98$ THz [8], [10], while for $N=10^{18}$ $\mathrm{cm}^{-3}$, $\Gamma_n=4$ THz [12]. $\Gamma_d$ is a critical parameter that drives the Si THz response through the denominator in (1) because $f<\Gamma_d$. To model $\Gamma_d$ for arbitrary doping level and type, we interpolate literature data [8]–[12] of a number of values $\mu$d and $N$. In the far-infrared range, $\Gamma_d$ becomes negligible relative to $f$, and SPs propagating on heavily doped Si are well confined at the interface and suffer a weak attenuation [24].

Due to the large values of $\varepsilon_\infty$ and $\Gamma_d$, the necessary condition of SP existence in the THz range is more complicated than for metals, for which it simply writes $\omega<\omega_p/\sqrt{2}$ [25]. For highly doped semiconductors, from the condition $n_{\mathrm{SP}}(f)>1$ and from (1), one obtains

$$f<f_l(N)=\sqrt{\frac{f_p^2(N)}{\varepsilon_\infty+1/2}-\Gamma_d^2}. \tag{2}$$

For frequencies larger than $f_l(N)$, it is not possible for a SP to propagate over the doped semiconductor. The limit frequency value $f_l(N)$ is plotted in Fig. 1 versus $N$ for $d=n$ and $p$ doping types, together with the plasma frequency $f_p(N)$. Hence for $N=3\times10^{17}$ $\mathrm{cm}^{-3}$, SP can exist only at low frequencies (<0.5 THz), while, for $N=10^{18}$ $\mathrm{cm}^{-3}$, SPs are supported up to 3 THz.

The SP wave vector is

$$k_{SP}(f)=k_0(f)\sqrt{\frac{\varepsilon(f)}{\varepsilon(f)+1}} \tag{3}$$

with $k_0(f)=2\pi\,f/c$. We define the SP absorption coefficient as $\alpha_{SP}(f)=2\mathrm{Im}(k_{SP}(f))$ and the SP refraction index as $n_{SP}(f)=\mathrm{Re}(k_{SP}(f)/k_0(f))$. Both $\alpha_{SP}(f)$ and $n_{SP}(f)$ are plotted in Fig. 2 for different doping levels.

Absorption forbids SP propagation on doped semiconductors over more than a few centimeters, and thus SP absorption limits the observable bandwidth rather than the SP coupling configuration. The other important SP feature is its refraction index $n_{\mathrm{SP}}$. Refraction index value close to unity means bad localization and

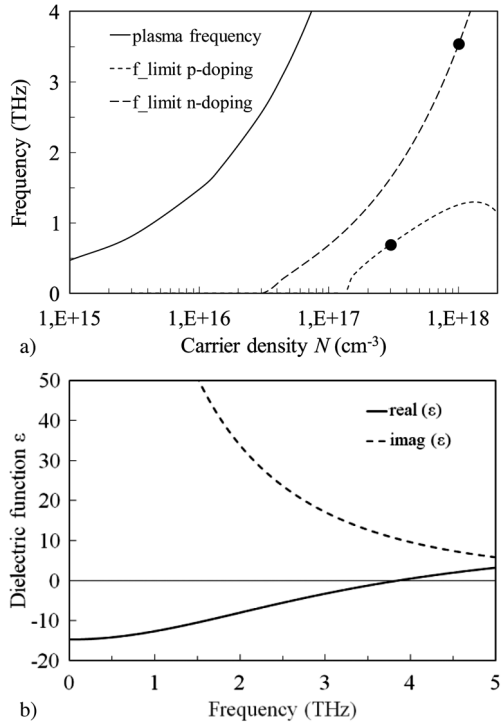


Fig. 1. (a) Plasma frequency $f_p(N)$ and limit frequency $f_l(N,d)$ versus carrier concentration $N$ for $n$-type and for $p$-type doped Si. (b) Drude model dielectric function for $n$-doped Si ($N=10^{18}$ $\mathrm{cm}^{-3}$).

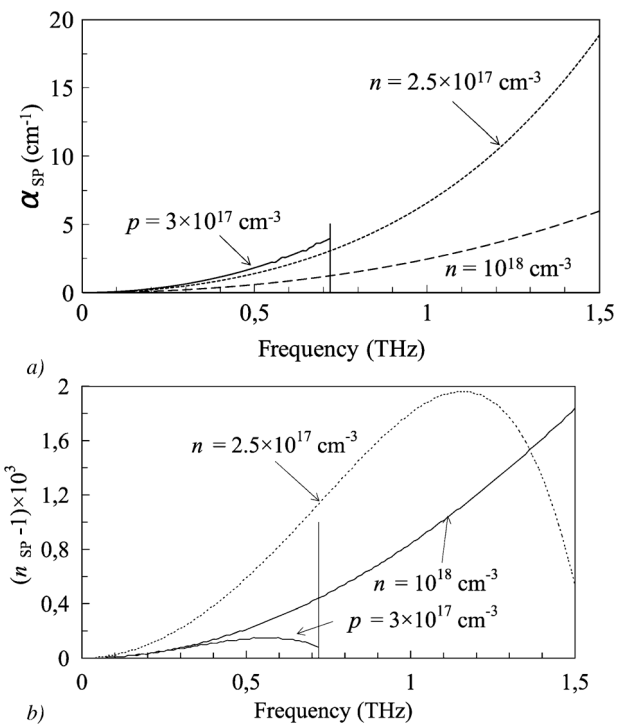


Fig. 2. (a) SP absorption and (b) refraction frequency dependencies, calculated from the Drude model for the sample-1 ($p=3\times10^{17}$ $\mathrm{cm}^{-3}$,), sample-2 ($n=10^{18}$ $\mathrm{cm}^{-3}$,) and for an intermediate case ($n=2.5\times10^{17}$ $\mathrm{cm}^{-3}$). The limiting frequency $f_l$ for sample-1 is marked by a vertical line.

considerable radiation losses, like in the case of metals [30]. The more $n_{\rm SP}$ exceeds the unity, the more field penetrates into the substrate, increasing surface sensitivity and field confinement, but on the other hand SP absorption increases as well. The value $n_{\rm SP} = 1.001$ is a reasonable compromise between a sufficiently large propagation length $L_{\rm SP}$ ($L_{\rm SP} = 1/\alpha_{\rm SP} = 1 \sim 3$ cm) and a good field localization ($d_{\rm air} = (k_0\sqrt{n_{\rm SP}^2 - 1})^{-1} = 5 \sim 1$ mm). In Si, these considerations determine the optimal carrier concentration and type of doping to observe and characterize SP, i.e., $N = 10^{18}$ cm$^{-3}$ and $p$-doping. Actually, Si is not the best semiconductor to deal with THz SP because of its low mobility value. InSb is definitively a better material ($\mu = 4.4 \times 10^4$ cm$^2$/(V$\cdot$s) [26], i.e., $\Gamma = 0.02$ THz): hence, for $N = 10^{17}$ cm$^{-3}$, $n_{\rm SP} = 1.05$ and SP absorption is still low, resulting in propagation length $L_{\rm SP} = 3$ cm and in a good field confinement ($d_{\rm air} = 0.1$ mm at 1 THz) for InSb.

## III. Sample Characterization

In our study, we used two highly doped 0.3-mm-thick Si samples: Sample-1 is a $<100>$ Si wafer $p$-doped with bore, whose resistivity is $R_1 = 0.08 \sim 0.1$ Ωcm; Sample-2 ($<111>$ orientation) is $n$-doped with phosphor, and its resistivity is $R_2 = 0.009 \sim 0.011$ Ωcm. We also used metal samples (aluminium, copper, and gold) as an example of known material. The Si sample carrier concentration $N$ was estimated from the supplied dc resistivity $R$: $N_1 = (3 \pm 1) \times 10^{17}$ cm$^{-3}$, $N_2 = (1 \pm 0.5) \times 10^{18}$ cm$^{-3}$, while for the metal it is known to be about $N_3 = 10^{23}$ cm$^{-3}$.

We characterized the THz properties of our sample using a classical THz time-domain spectroscopy system already described in [27] and [28]. At the sample location, the THz beam is almost parallel with a 15-mm diameter and it is p-polarized.

For doping level higher than $10^{17}$ cm$^{-3}$, THz transmission amplitude $T$ is very weak. For sample-1, we measured $T = 10^{-2} \sim 10^{-4}$ for $f = 0.03 \sim 0.3$ THz by THz-TDs and, using a FTIR spectrometer, $T^2 > 10^{-3}$ for $f > 8$ THz. A reflection spectrum is more informative but not very sensitive to the dielectric function value; moreover, reflection provides information only about the surface region and not about the bulk properties. By fitting the measured reflection spectra in the 0.1–3-THz frequency range, we estimated, for sample-1, $\Gamma_p = 2 \pm 0.5$ THz, and $\Gamma_n = 3.5 \pm 0.5$ THz for sample-2. Within these large uncertainties, we obtain a reasonable agreement with data evaluated from dc resistivity or already published [7], [8], [10], [12], [15]. These values were used to calculate the Si dielectric function from relation (1) [see Fig. 1(b)]and the SP properties from (3).

Let us point out here the advantage of dealing with SP in order to characterize the doped semiconductor material. It originates in the much longer interaction length $L$ with the material as compared to simple reflectometry. For example, for $N = 10^{18}$ cm$^{-3}$ and $L = 3$ cm, an increase of $N$ or $\Gamma$ by 10% will increase the SP amplitude after propagation over the length $L$ by 20% [cf. (4)], while the corresponding change in reflectivity is only 1%. For higher then $N = 10^{18}$ cm$^{-3}$ doping levels, just longer propagation distance should be used to obtain good sensitivity.

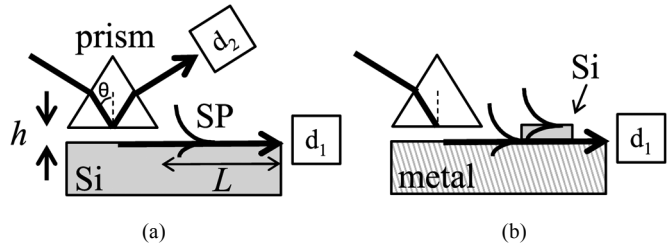


Fig. 3. Scheme of the SP propagation experiments. The right scheme is related to our new method of SP parameter study (see text). $d_1$ (transmission) and $d_2$ (reflection) are THz detectors.

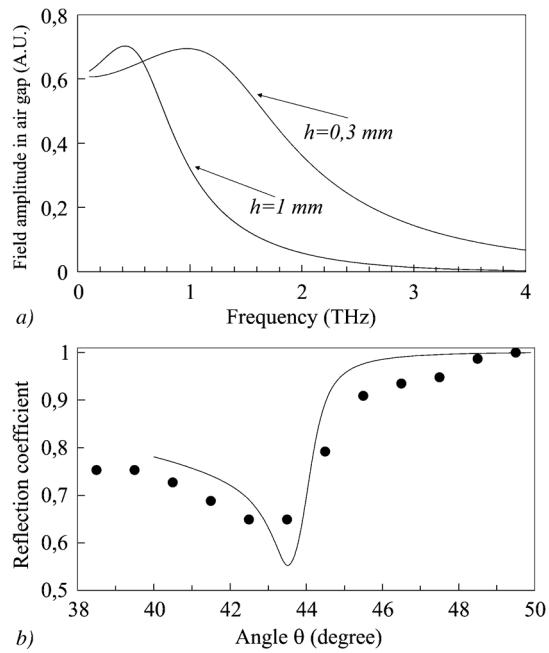


Fig. 4. (a) Calculated SP amplitude inside the ATR air gap for $h = 1$ mm (dashed line) and $h = 0.3$ mm (solid line) with sample-2. The angle of incidence is 44°. (b) ATR reflected signal, integrated over the 0.1–1.2 THz experimental frequency range, versus the angle of incidence $\theta$—measured (circles) and calculated (solid line)-for sample-2 and $h = 0.5$ mm.

## IV. Excitation and Study of SP in ATR Scheme

First, we excited SP using an ATR scheme [Fig. 3(a)], commonly used in the visible range [25] arranged in the Otto configuration [28]. The prism (right angle at the apex) is made in Teflon ($n_{\rm prism} = 1.432$ over the whole studied THz range).

The angle of incidence $\theta$ is determined from parallel wave vector conservation: $n_{\rm prism} k_0 \sin(\theta) = n_{SP} k_0$. In our case, dispersion of both $n_{\rm prism}$ and $n_{\rm SP}$ is negligible, thus SP can be excited at a single angle value over a broad frequency range (see Fig. 4). At this angle, because SP excitation occurs over a limited area and because of losses, the signal reflected by the prism should 0exhibit a dip. This is clearly observed in the experimental record: Fig. 4(b) shows the spectrally integrated THz TDS signal measured versus incident angle using a goniometric THz-TDS setup. The agreement with the calculated curve is fairly good, the differences may originate from the plane wave hypothesis in the modeling, or from a deviation from the Drude model. The experimental value of the optimal angle is $\theta = 44 \pm 1°$, which is 0.5° smaller than the theoretical prediction, and the measured SP angular width is twice the calculated one, which means that the SP losses are bigger than expected.

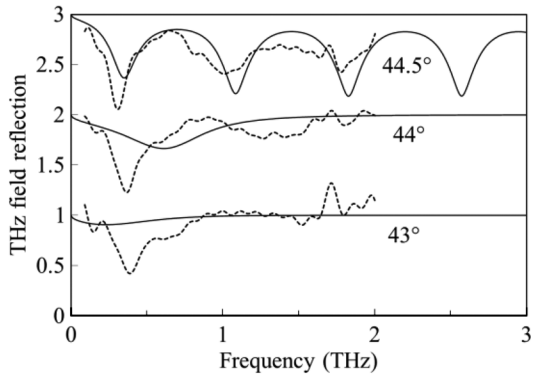


Fig. 5. Attenuated total reflection spectra for different incident angles (dashed line = measured; solid line = calculated). The air gap is $h = 1$ mm. The 44° and 44.5° curves are offset by $+1$ and $+2$ for sake of clarity.

We measured and calculated the ATR reflectivity spectra for sample-2. Let us notice that a deep in reflection is not always related to SP excitation, but may result from interferences of the incoming beam inside the air gap [17]. An example of this artifact is presented in Fig. 5 for $\theta = 44.5°$. SP resonance is around 0.4 THz, as expected for all of the experimental angles. While detector $\mathrm{d}_2$ records spectral dips, detector $\mathrm{d}_1$ recorded broadband SP signal from 0.2 till 0.7 THz [31].

Optimal frequency is determined mostly by the air gap ($h = 1$ mm corresponds to $f = 0.4$ THz), but also at second order by the incidence angle. Fig. 4(a) confirms that, for sample 1 and $h = 1$ mm, SP is excited at 0.4 THz (maximum of the curve). Moreover, Fig. 4(b) shows that this SP is excited all over the range $\theta \sim 41° \sim 45°$. For 44.5° in Fig. 5, the SP resonance is hidden by interferences due to a Fabry–Pérot effect in the air gap. Calculated curves in Fig. 5 shows that the SP optimal frequency should slightly decrease with $\theta$, which is not experimentally observed. This is maybe related to discrepancy between the Drude model and the actual THz response of the metal surface.

## V. SP Observation in Propagation Configuration

To measure with a better precision the SP propagation properties, we employ the ATR prism as a localized coupler which permits to excite a SP propagating at the sample-air interface. This SP is received by a detector located at the edge of the sample ($\mathrm{d}_1$ in Fig. 3). The distance $L$ between the prism and the sample edge could be varied from 1 to 5 cm, without affecting the coupling and detection efficiencies. The influence of the freely propagating wave is reduced by a screen above the surface. To be sure that the SP wave dominates in the detected signal, we also delayed SP by 10-$\mu$m-thick and 10-mm-long polyethylene film on the sample surface, as such film does not delay freely propagating waves. We have already demonstrated the efficiency of this scheme in the case of SP propagating on metals [28]. The signal received by the detector is proportional to the SP field at distance $L$

$$S(f,L) \propto E_{\mathrm{SP}}(f,L) = E_{\mathrm{SP}}(f,0)\exp\left(i\left[k_{\mathrm{SP}}(f,N,\Gamma) - k_0(f)\right]L\right). \quad (4)$$

Two records are performed, at two different distances $L_1$ and $L_2$ such as $\Delta L = L_2 - L_1$. The ratio of both records allows us to get rid of the coupling and detecting coefficients. We obtain

$$T(f,\Delta L) = \frac{S(f,L_2)}{S(f,L_1)} = \exp\left(i\left[k_{\mathrm{SP}}(f,N,\Gamma) - k_0(f)\right]\Delta L\right). \quad (5)$$

This transmission spectrum is rather sensitive to the material properties thanks to the large interaction length $\Delta L$. From (5), we easily derive the SP propagation parameters

$$\begin{cases} \alpha_{\mathrm{SP}}(f) = 2\mathrm{Im}(k_{\mathrm{SP}}) = 2\frac{\ln|T(f,\Delta L)|}{\Delta L} \\ n_{\mathrm{SP}}(f) = \frac{\mathrm{Re}(k_{\mathrm{SP}})}{k_0} = 1 + \frac{c}{2\pi f} \times \frac{\arg(T(f,\Delta L))}{\Delta L}. \end{cases} \quad (6)$$

The handicap of this method is that the distance between the THz source and detector is changed, so the phase of the signal is badly determined. To validate our results, we replaced the sample by a metallic slab, and we compared our data for metal with already published ones [30]. In addition, we performed a second experiment inspired from [32]. We employ the ATR prism to excite a SP on an aluminum substrate, and we detect the SP at the edge of the substrate, as previously described. However, now a thin Si sample is placed over the metal in between the prism and the edge of the substrate (Fig. 3 right). The SP propagating over the metal impinges the Si sample and then propagates over this sample. However, the 0.3-mm-thick Si sample is thinner than the SP decay length in air ($d_{\mathrm{air}} \approx 1$ mm), which permits a good coupling between the SP propagating over the metal and over the Si sample. On the other hand, the Si sample is much thicker than the SP decay length in doped-Si (typically 60 $\mu$m at 1 THz), and thus it could be considered as a semi-infinite medium for the SP propagating over it. In this configuration, the THz source and detector are kept steady: the reference is obtained with the bare metal, while the signal is recorded with the Si sample over the metal. This allows us to precisely determine the SP refractive index. On the other hand, because of losses due to diffraction of the SP wave at both the front and rear edges of the Si sample, SP absorption is only approximately obtained.

In fact, both methods provide us with similar spectra, therefore we present below an average of the values measured via both methods, for $L = 1$, 3 and 5 cm. The absorption $\alpha_{\mathrm{SP}}$ as well as the effective index $n_{\mathrm{SP}}$ of the SP propagating over samples 1 and 2, and over aluminum, are plotted in Fig. 6(a) and (b), respectively.

The method accuracy is tested on the example of Al surface. Resulting value of SP absorption coefficient on Al (for $\mathrm{f} = 1$ THz) is $\alpha_{\mathrm{SP}} = 0.1 \pm 0.05\ \mathrm{cm}^{-1}$, $\mathrm{Lx} = 5 \pm 2$ cm, $\mathrm{n} = 1.002 \pm 0.001$ That is comparable to published data of several independent groups: Geong *et al.* in [30] and in [33] for Al published data that corresponds at 1 THz to $\alpha_{\mathrm{SP}} = 0.02\ \mathrm{cm}^{-1}$ and $\mathrm{n} = 1.01$. Nahata *et al.* in [34] for Al at 1 THz published $\mathrm{L_x} = 8$ cm, $\mathrm{L_z} = 2$ mm, $\varepsilon = -690 + \mathrm{i} * 455$, $\mathrm{n} = 1.0004$. Gerasimov *et al.* in [35] for Au and $\mathrm{f} = 2.18$ THz published $\mathrm{L_x} = 3$ cm.

For the doped Si, the Drude model gives a good estimation of the measured values only in the case of SP absorption

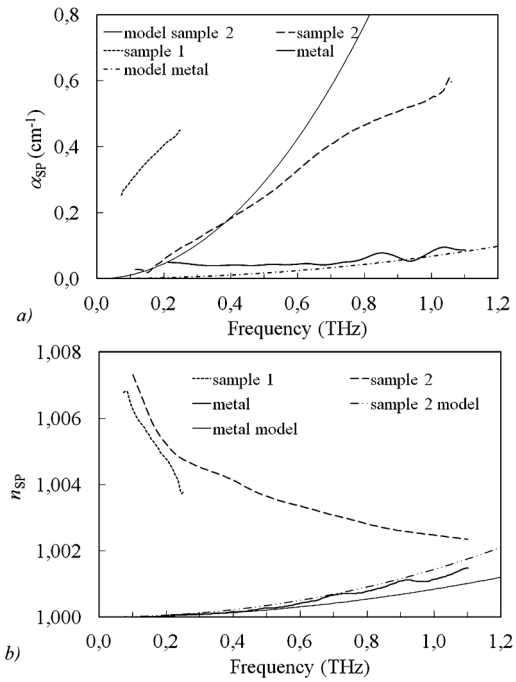


Fig. 6. SP absorption and effective index spectra, for samples 1, 2 and metal (aluminum), extracted from the propagation measurements. The calculated curve for sample 2 and for Al, based on the Drude model, are also plotted.

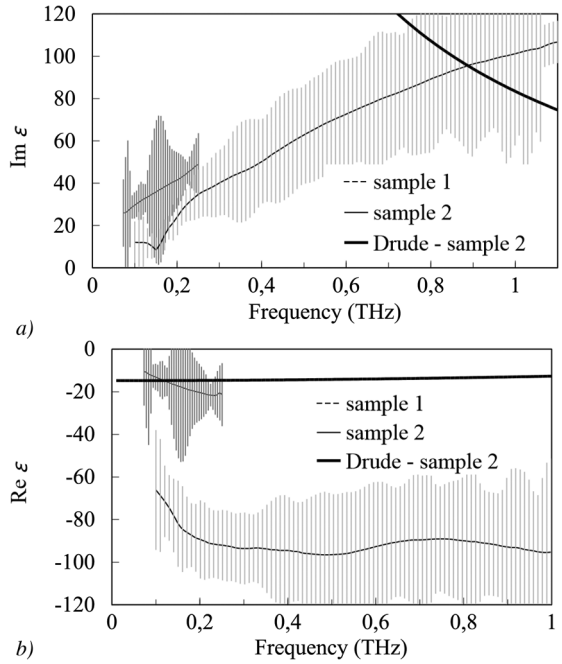


Fig. 7. (a) Imaginary and (b) real parts of the surface dielectric function of doped Si, together with error bars. The Drude model value for sample 2 is also plotted (double line).

[Fig. 6(a)]. Very surprisingly, the Drude model does not fit at all the experimental results for the refractive index. For doped Si, not only the values differ in magnitude, but the variation with frequency of the calculated and measured curves are opposite. All these experimental results tend to indicate that the region at the Si surface is less doped than it is actually. Of course, a natural oxide layer exists at the Si surface, but its interaction with the THz waves may be neglected because of its nanometric thickness.

Then we evaluated the dielectric function of doped Si from the SP complex effective index, which is written as

$$\varepsilon(f) = \frac{\tilde{n}_{\mathrm{SP}}(f)^2}{1 - \tilde{n}_{\mathrm{SP}}(f)^2} \tag{7}$$

with $\tilde{n}_{\mathrm{SP}}(f) = n_{\mathrm{SP}}(f) + i\alpha_{\mathrm{SP}}(f)c/(4\pi f)$. Small changes of $n_{\mathrm{SP}}(f)$ relative to unity are very critical, because of the denominator in (7). Similarly, small errors in $n_{\mathrm{SP}}$ lead to large errors in the so-achieved dielectric function $\varepsilon$. From (7) and the data shown in Fig. 6, we obtain the doped-Si dielectric function plotted in Fig. 7.

The imaginary part of the dielectric function of the two doped-Si samples differ strongly from the Drude model (for sake of legibility, only the Drude model corresponding to sample 2 is plotted in Fig. 7). In addition, the variation of the curves with frequency is opposite. The measured one increases with frequency, while the calculated one decreases. For the real parts, the discrepancies in slopes are not so pronounced, but the absolute value for sample 2 is approximately five times bigger than the calculated one.

This surprising observation, which is confirmed by each of the methods we employed in this study, has to be related to the shorter-than-expected SP propagation length on metals [32]–[35]. Today, no definitive explanation of this phenomenon is satisfactory. Contrary to metals that could suffer from oxidation or water/pollutants adsorption at the surface, Si is more chemically stable. In addition, because of the smaller free carrier density of our samples as compared to metal, the SP field penetrates relatively deeply in the semiconductor and thus is less sensible to what occurs within a nanometer at the surface. Thus a possible explanation could be the nonlocal behavior of the carrier in the surface selvedge, which leads to anomalous skin effect [36], a well-known phenomenon in the microwave domain. Further experimental and theoretical developments are compulsory to validate this explanation or any other one [5].

## VI. Conclusion

We applied several methods to determine the far infrared properties of highly doped Si surface. As classical techniques, either THz-TDS in reflection or ATR, are not enough sensitive to determine a precise value of the THz dielectric function of doped-Si, we measured the propagation properties of SP over long distances. The longer propagation distance, i.e. the longer interaction of the THz SP wave with the substrate material, makes the technique very sensitive and accurate. Simultaneously, we solved the problem of phase in such measurements by using a complementary SP propagation technique, in which the doped-Si sample is put over a metal sample. All of these different techniques allowed us to obtain the complex dielectric function of doped-Si over the THz frequency range. This experimentally determined values differ strongly to the values

calculated from the Drude model. Not only the measured values are typically one order of magnitude larger than the calculated ones, but also they show an opposite behavior with frequency. It seems that the dielectric function of highly doped Si at the surface is different from the bulk value in the THz range. This could be related to similar observations with metal substrates, for which the SP propagation length is more than one order of magnitude than the calculated one. A possible explanation, which should be validated by complementary works, could be a nonlocal behavior of the free charges in the vicinity of the sample surface. Let us also notice that classical THz-TDS measurements are more sensitive to the bulk value of the doped-Si dielectric function, and thus lead to results in good agreement with the Drude model or models extrapolated from the Drude theory [2], [3], [5], [6], while SP test mostly the surface region (between 0 and a few tens of micrometers) of the material.

## REFERENCES


[1] M. A Ordal, L. L. Long, R. J. Bell, S. E. Bell, R. R. Bell, R. W. Alexander, Jr., and C. A. Ward, "Optical properties of the metals Al, Co, Cu, Au, Fe, Pb, Ni, Pd, Pt, Ag, Ti, W in the infrared and far infrared," *Appl. Opt.*, vol. 22, pp. 1099–1119, Apr. 1983.

[2] M. van Exter and D. Grischkowsky, "Carrier dynamics of electrons and holes in moderately-doped silicon," *Phys. Rev. B*, vol. 41, pp. 12140–12149, Jun. 1990.

[3] T.-I. Jeon and D. Grischkowsky, "Characterization of optically dense, doped semiconductors by reflection THz time domain spectroscopy," *Appl. Phys. Lett.*, vol. 72, pp. 3032–3034, Jun. 1998.

[4] J. Lloyd-Hughes, "Generalized conductivity model for polar semiconductors at terahertz frequencies," *Appl. Phys. Lett.*, vol. 100, pp. 122103–122103, Mar. 2012.

[5] J. Lloyd-Hughes and T.-I. Jeon, "A review of the terahertz conductivity of bulk and nano-materials," *J. Infrared Milli. Terahz. Waves*, vol. 33, pp. 871–925, Sep. 2012.

[6] K. J. Willis, S. C. Hagness, and I. Knezevic, "Terahertz conductivity of doped silicon calculated using the ensemble Monte Carlo/finite-difference time-domain simulation technique," *Appl. Phys. Lett.*, vol. 96, Febr. 2010, Art. ID 062106.

[7] K. J. Willis, S. C. Hagness, and I. Knezevic, "A global EMC-FDTD simulation tool for high-frequency carrier transport in semiconductors," in *Proc. 13th Int. Workshop Computational Electron.*, Beijing, China, May 27–29, 2009, pp. 1–4.

[8] T.-I. Jeon and D. Grischkowsky, "Nature of conduction in doped silicon," *Phys. Rev. Lett.*, vol. 78, pp. 1106–1109, Febr. 1997.

[9] F. Garet, L. Duvillaret, and J.-L. Coutaz, "THz time-domain spectroscopy of nanometric-thick gold layers," in *Proc. IRMMW*, 2004, p. 467.

[10] N. Laman and D. Grischkowsky, "Terahertz conductivity of thin metal films," *Appl. Phys. Lett.*, vol. 93, 2008, Art. ID 051105.

[11] S. Nashima, O. Morikawa, K. Takata, and M. Hangyo, "Measurement of optical properties of highly doped silicon by terahertz time domain reflection spectroscopy," *Appl. Phys. Lett*, vol. 79, pp. 3923–3925, Dec. 2001.

[12] T. Nagashima and M. Hangyo, "Measurement of complex optical constants of a highly doped Si wafer using terahertz ellipsometry," *Appl. Phys. Lett.*, vol. 79, pp. 3917–3919, 2001.

[13] *Terahertz Optoelectronics*, K. Sakai, Ed. Berlin: Springer-Verlag, 2005, pp. 203–271.

[14] S. L. Katz, "Near terahertz silicon conductivity measurements via high Q resonant cavity," Univ. Wisconsin-Madison, 2010, MS report (unpublished).

[15] B. B. Yang, S. L. Katz, K. J. Willis, M. J. Weber, I. Knezevic, S. C. Hagness, and J. H. Booske, "A high-Q terahertz resonator for the measurement of electronic properties of conductors and low-loss dielectrics," *IEEE THz Sci. Technol.*, vol. 2, pp. 449–459, 2012.

[16] J. Gomez Rivas, M. Kuttge, P. Haring Bolivar, H. Kurz, and J. A. Sanchez-Gil, "Propagation of surface plasmon polaritons on semiconductor gratings," *Phys. Rev. Lett.*, vol. 93, 2004, Art. ID 256804.

[17] H. Hirori, M. Nagai, and K. Tanaka, "Destructive interference effect on surface plasmon resonance in terahertz attenuated total reflection," *Opt. Exp.*, vol. 13, 2005, Art. ID 10801.

[18] S.-Z. A. Lo and T. E. Murphy, "Terahertz surface plasmon propagation in nanoporous silicon layers," *Appl. Phys. Lett.*, vol. 96, 2010, Art. ID 201104.

[19] T. H. Isaac, W. L. Barnes, and E. Hendry, "Determining the terahertz optical properties of subwavelength films using semiconductor surface plasmons," *Appl. Phys. Lett.*, vol. 93, 2008, Art. ID 241115.

[20] T. H. Isaac, J. Gómez Rivas, J. R. Sambles, W. L. Barnes, and E. Hendry, "Surface plasmon mediated transmission of subwavelength slits at THz frequencies," *Phys. Rev. B*, vol. 77, 2008, Art. ID 113411.

[21] R. Soref, R. E. Peale, and W. Buchwald, "Longwave plasmonics on doped silicon and silicides," *Opt. Exp.*, vol. 16, pp. 6507–6514, 2008.

[22] E. Hendry, F. J. Garcia-Vidal, L. Martin-Moreno, J. Gómez Rivas, M. Bonn, A. P. Hibbins, and M. J. Lockyear, "Optical control over surface-plasmon-polariton-assisted THz transmission through a slit aperture," *Phys. Rev. Lett.*, vol. 100, 2008, Art. ID 123901.

[23] K. J. Willis, J. S. Ayubi-Moak, S. C. Hagness, and I. Knezevic, "Global modeling of carrier-field dynamics in semiconductors using EMC-FDTD," *J. Comput. Electron.*, 2009, DOI 10.1007/s10825-009-0280-4.

[24] J. C. Ginn, R. L. Jarecki, Jr., E. A. Shaner, and P. S. Davids, "Infrared plasmons on heavily-doped silicon," *J. Appl. Phys.*, vol. 110, 2011, Art. ID 043110.

[25] S. A. Maier, *Plasmonics: Fundamentals and Applications*. Berlin, Germany: Springer Science+Business Media LLC, 2007.

[26] Y. Zhang, A. Berrier, and J. Gomez Rivas, *Chinese Opt. Lett.*, vol. 9, p. 110014, 2011.

[27] M. M. Nazarov, A. P. Shkurinov, A. A. Angeluts, and D. A. Sapozhnikov, "On the choice of nonlinear optical and semiconductor converters of femtosecond laser pulses into terahertz range," *Radiophys. Quantum Electron.*, vol. 52, pp. 536–545, 2009.

[28] M. M. Nazarov, E. A. Bezus, and A. P. Shkurinov, "Thin and thick dielectric films for THz surface plasmon control," *Laser Phys.*, vol. 23, 2013, Art. ID 056008.

[29] K. Kurosawa, R. M. Pierce, S. Ushioda, and J. C. Hemminger, "Raman scattering and attenuated-total-reflection studies of surface-plasmon polaritons," *Phys. Rev.*, vol. B33, pp. 789–798, 1986.

[30] M. Gong, T.-I. Jeon, and D. Grischkowsky, "THz surface wave collapse on coated metal surfaces," *Opt. Exp.*, vol. 17, 2009, Art. ID 17088.

[31] M. Nazarov, A. Shkurinov, F. Garet, and J.-L. Coutaz, "Characterization Of highly doped Si with surface plasmon," in *Proc. IRMMW-THz*, Sep. 1–6, 2013, paper Tu12-3.

[32] J. F. O'Hara, R. D. Averitt, and A. J. Taylor, "Prism coupling to terahertz surface plasmon polaritons," *Opt. Exp.*, vol. 13, pp. 6117–6126, 2005.

[33] T.-I. Jeon and D. Grischkowsky, "THz Zenneck surface wave THz surface plasmon propgation on a metal sheet," *Appl. Phys. Lett.*, vol. 88, 2006, Art. ID 061113.

[34] S. Pandey, S. Liu, B. Gupta, and A. Nahata, "Self-referenced measurements of the dielectric properties of metals using terahertz time-domain spectroscopy via the excitation of surface plasmon-polaritons," *Photon. Res.*, vol. 1, pp. 148–153, Nov. 2013.

[35] V. V. Gerasimon, B. A. Knyazev, I. A. Kotelnikov, A. K. Nikitin, V. S. Cherkassky, G. N. Kulipanov, and G. N. Zhizhin, "Surface plasmon polaritons launched using a terahertz-free-electron laser: Propagation along a gold–ZnS–air interface and decoupling to free waves at the surface edge," *J. Opt. Soc. Amer. B*, vol. 30, pp. 2182–2190, Aug. 2013.

[36] G. E. H. Reuter and E. H. Sondheimer, "The theory of the anomalous skin effect in metals," *Proc. Royal Soc. London*, vol. A195, pp. 336–364, 1948.

[37] M. Gong, T.-I. Jeon, and D. Grischkowsky, "THz surface wave collapse on coated metal surfaces," *Opt. Exp.*, vol. 17, pp. 17088–17101, 2009.

[38] D. L. Begley, R. W. Alexander, C. A. Ward, R. Miller, and R. J. Bell, "Propagation distances of surface electromagnetic waves in the far infrared," *Surface Sci.*, vol. 81, pp. 245–251, 1979.

[39] J. Saxler, J. Gomez Rivas, C. Janke, H. P. M. Pellemans, P. Haring Bolivar, and H. Kurz, "Time-domain measurements of surface plasmon polaritons in the terahertz frequency range," *Phys. Rev. B*, vol. 69, 2004, Art. ID 155427.

[40] M. M. Nazarov, F. Garet, D. Armand, A. Shkurinov, and J.-L. Coutaz, "Surface plasmon THz waves on gratings," *C. R. Physique*, vol. 9, pp. 232–247, 2008.

**Maxim M. Nazarov** was born in USSR in 1976. He received the Ph.D. degree in physics from the M.V.Lomonosov Moscow State University, Moscow, Russia, in 2002. His dissertation was on the topic of surface plasmon enhanced optical harmonics on metal grating.

He was a Scientific Researcher with MSU till 2012, working on the topics of femtosecond lasers and THz spectrosscopy. In 2012 he has been a Scientific Researcher with the Institute on Laser and Information Technologies, Russian Academy of Sciences, Shatura, working on the topic of polymer waveguides for THz and visible ranges, nanoparticles and integrated optics.

**Alexander P. Shkurinov** received the Ph.D. degree and Doctor of Physics and Math Sciences (Habilitation) from M.V. Lomonosov Moscow State University, Moscow, Russia, in 1988 and 2013, respectively.

He is a Professor with the Department of Physics and International Laser Center of M.V. Lomonosov Moscow State University (MSU), Moscow, Russia, Head of the Laboratory of Terahertz Optoelectronics and Spectroscopy at MSU. His research interests are in the applications of picosecond and femtosecond laser techniques for time-resolved spectroscopy of various objects including complex molecules. He was the first one to experimentally develop and apply Coherent Antistokes Raman Spectroscopy (CARS) technique to the study of biological molecules. He has authored and coauthored more than 150 papers in peer-reviewed scientific journals, was invited to deliver more than 60 invited lectures and talks, organizes annually well-recognized international conferences (TERA, LALS), and is a committee member of seven other international scientific meetings. He has been an Invited Professor with the University of Littoral, Dunkerque, France (1996–2000), a Research Fellow with the University of Twente, Enschede, The Netherlands (1995–1996), and an Invited Professor with the University Bordeaux I, Bordeaux, France (1993).

Prof. Shkurinov was the recipient of the Russian Optical Society Award, the Medal in honor of Prof. Rozhdestvensky, for the contribution into the development of optical science and technology (2008) and the Diploma with honor from the Department of Physics of MSU (1985).

**Frédéric Garet** was born in France in 1969. He received the Ph.D. degree in physics from the Technological University of Grenoble, Grenoble, France, in 1997.

In October 1998, he joined the IMEP-LAHC Laboratory at the University of Savoy, Chambery, France, where he is an Associate Professor. His current research interests include terahertz spectroscopy of materials, devices characterization, and THz generation and detection

**Jean-Louis Coutaz** received the Ph.D. degree from the University of Grenoble, Grenoble, France, in 1981, and the Docteur d'Etat degree from the Polytechnic University of Grenoble, Grenoble, in 1987. His Ph.D. dissertation was on ion-exchange in glass and the Docteur d'Etat dissertation was on the subject of the generation of second-harmonic waves at metallic grating surfaces.

In 1981–82, he served as a Lecturer with the University of Blida, Algeria, under a cooperation scheme. From 1983 to 1993, he was a full-time Researcher with the French CNRS, working on guided-wave nonlinear optics (second harmonic generation, Raman scattering, electrooptic modulation). During 1988–1989, he was a Postdoctoral Fellow with the Royal Institute of Technology (KTH), Stockholm, Sweden, where he worked on semiconductor doped glasses. In 1993, he became a Professor of physics with the University of Savoie, where he has started research activities in ultrafast optoelectronics. He was for several years director of the laboratory LAHC in the same university, and since 2007 he serves as deputy director of the IMEP-LAHC institute, a common laboratory of the Universities of Grenoble and Savoie. He was an Invited Professor with KTH Stockholm in 2000, and with Tohoku University, Sendaï, Japan, in 2013. His present research activities include terahertz time-domain spectroscopy, electro-optic sampling and ultrafast III-V semiconductor devices. He is the author and coauthor of approximately 500 papers and communications, and he was the editor of the book (in French) *THz Optoelectronics* (EDP Sciences, 2008).

Prof. Coutaz was the guest editor of special issues of the *IEE Proceedings* (vol. 81, 2002), and of Comptes-Rendus (Physique) [vol. 9 (2008) and vol. 11 (2010)]. He was the secretary of the French Optical Society (2005–2009). He is the member of the committee of several international conferences and of the editorial board of the *International Journal of Infrared, Millimeter and THz Waves*.